Atom Indonesia

Journal homepage: http://aij.batan.go.id

First Magnon of BATAN's Neutron Triple-Axis Spectrometer

I. Sumirat*

Center for Science and Technology of Advanced Materials, National Nuclear Energy Agency
Puspiptek Area, Serpong, Tangerang 15310, Indonesia

ARTICLE INFO

Article history:
Received 31 October 2015
Received in revised form 27 April 2016
Accepted 30 April 2016

Keywords:
BATAN
Inelastic neutron scattering
Triple axis spectrometer
Magnon

ABSTRACT

The National Nuclear Energy Agency of Indonesia (BATAN) has one dedicated spectrometer for inelastic neutron scattering experiments. The instrument is a thermal neutron triple-axis spectrometer known as SN1. SN1 was installed in 1992 in the experimental hall of G. A. Siwabessy Research Reactor, Serpong, Banten. Malfunctions of the hardware and software have prevented the instrument from performing inelastic scattering measurements since 1996. The 2011-2015 five years project has been initiated to revitalize and optimize the SN1. The project serves as a preparation for the utilization of SN1 for the investigation of lattice dynamics, spin wave and magnetic excitations in condensed matters that will be started in 2016. In 2013, SN1 has successfully been repaired and was able to measure phonon dispersion relation of available single crystals, *i.e*., Cu, pyrolytic graphite (PG), Ge, and Al. In 2015, the first experiment on magnetic excitation to investigate magnon dispersion relation of a known Fe single crystal has been carried out. Standard methods of inelastic scattering measurements, *i.e*., a constant-energy transfer $\hbar\omega$ with either fixed final neutron energy E_f = 14.7 meV or fixed incoming neutron energy E_i = 30.59 meV, and a constant momentum transfer **Q** with fixed incoming neutron energy E_i = 30.59 meV, were applied to measure the low-energy magnetic excitations. For fixed E_f measurement, a 5-cm thick PG filter was set between the sample and the analyzer to eliminate λ/n harmonics. To limit the energy and momentum spreads of the beam, collimations of 40 minutes were applied before and after the sample. The spin waves were measured along the three principal symmetry directions of [00ζ], [ζζ0], and [ζζζ]. The measured magnons were compared to values in reference and were found to be in a good agreement with them. With such accomplishments, we are convinced that SN1 is now ready for its inelastic scattering application and will become one of BATAN's neutron instrument which is routinely utilized for materials characterization on lattice dynamics and magnetic excitations by local and foreign scientists. Besides reporting the SN1 first measured magnon, the current status of SN1 instrument development will also be presented briefly.

INTRODUCTION

Since its invention more than 50 years ago, the neutron triple-axis spectrometer (TAS) is still part of standard equipment that is always present in every research reactor. The TAS is a very versatile inelastic neutron scattering instrument since it can observe energy excitations at almost any coordinate in the momentum transfer **Q** and energy E space. The principle work and detail of technical aspects of the TAS instrument can be found in [1]. The TAS is applied especially to investigate phenomena that involve energy excitations in condensed matter. Moreover, there are phenomena that can only be probed by TAS due to the unique characteristics of neutron during interaction especially with magnetic materials. Recent research on phenomena such as

*Corresponding author.
E-mail address: sumirat@batan.go.id
DOI: http://dx.doi.org/10.17146/aij.2016.510

quantum magnetism [2,3], high-T_c superconductor materials [4,5], frustrated magnets [6], energy/hydrogen storage [7-10], multiferroics [11], and protein dynamics [12,13] are some examples among other topics that apply inelastic neutron scattering to investigate many novel and interesting properties. As a national research institution, BATAN should also be involved in research activities on advanced materials that apply nuclear-based technique for their characterizations. This is in accordance with the vision of BATAN to become the center of excellence in nuclear-based research at both national and ASEAN regional levels. One of the missions that could be implemented is the application of neutron scattering technique for the investigation of lattice dynamics and magnetic excitations in condensed matter.

This work is a part of the 2011-2015 projects to revitalize and optimize the SN1 as the only neutron instrument available in BATAN for inelastic scattering experiments. In an attempt to test the newly-developed hardware and software, a series of experiments on lattice dynamics of several known samples were performed. In 2013, the first inelastic scattering data, *i.e*., the phonon dispersion relation of Cu, pyrolytic graphite (PG), Ge, and Al single crystals, were reproduced. The phonon data obtained are in good agreement with references.

This paper serves as a report of the first success of BATAN's neutron TAS in measuring magnetic excitation after it has undergone a major rebuild from very long idle since its installation. The author realizes that there are no novelties in the whole aspect of the instrument used, the technique of measurements applied, and characteristics of the material used as the sample. Nevertheless, the author is convinced that results of the present work can be considered as a first important step toward the utilization of BATAN's neutron TAS for research activities on the investigation of lattice dynamics and magnetic excitations in condensed matters. Through this publication, the author hopes to receive constructive comments from, and exchange discussion with, the relevant community regarding the quality and performance of the SN1 instrument, what scientific works the instrument can tackle, and what best things should be done for further development of the instrument.

EXPERIMENTAL METHODS

Instrument

The instrument is the SN1, a standard neutron triple axis spectrometer. The SN1 uses thermal neutrons emanating from the core of the G. A. Siwabessy research reactor. The beam tube number 4 (S4) is used to deliver the thermal neutrons from the core to the instrument. The dimension of effective polychromatic beam size is 35 mm × 55mm ($W \times H$). The mononchromator is a flat PG(002) single crystal with a dimension of 50 mm × 70 mm × 10 mm ($W \times H \times T$). The analyzer is also a flat PG(002) single crystal with a dimension of 50 mm × 70 mm × 2 mm ($W \times H \times T$). The neutron sense is Left-Right-Left (W configuration). To limit the neutron beam divergence, a collimation system of Open - 40' - 40' - Open was applied. The area of incident beam slit of 16 mm (horizontal) × 30mm (vertical) and scattered beam slit of 20 mm (horizontal) × 40 mm (vertical) were set to decrease the background. For experiments with fixed final neutron energy, a PG filter of 50 mm thickness was placed after the sample to cut off the energy of neutron harmonics. The experiments were performed at room temperature and an external magnetic field of zero Tesla.

Sample

The sample is a *bcc* Fe single crystal with a purity of 99.994%, mosaicity of less than 0.1°, and dimension of 10 × 10 × 10 mm^3, provided by Princeton Scientific Corporation. Elastic scattering measurements were performed to determine two orthogonal Bragg vectors, *i.e*., Fe[110] and Fe[002]. The two vectors construct a scattering plane and serve as a horizontal plane for inelastic scattering measurements. The sample was mounted on the sample goniometer and aligned so that the (110) plane is parallel with the plane of the sample lower goniometer, *sgl - sample goniometer lower*. The two sets of the instrument coordinates of each Bragg peak were respectively obtained by performing iteration of scans and optimizations of the sample crystal scattering angle θ_s, take-off angle $2\theta_s$, upper *sgu - sample goniometer upper* and lower *sgl* tilting angles. The crystal structure and lattice parameters of the sample were taken from reference [14]. Instrument configuration, lattice parameters of the monochromator and analyzer, lattice constant of the sample, and the two sets of optimized instrument coordinates of the two vectors previously obtained were used to calculate the UB matrix of the sample-instrument particular configuration. The UB matrix combined with the choice of mode of excitation (longitudinal or transverse), position of the chosen Brillouin zone center, and the direction [*hkl*] of measurements in reciprocal space of the sample was

applied to transform the coordinates of reciprocal space of the sample i.e. (h, k, l, $\boldsymbol{Q}$, E) into the coordinate of the instrument i.e. (θ_m, $2\theta_m$, θ_s, $2\theta_s$,θ_a, $2\theta_a$, sgl, sgu) and vice versa to spot peaks of magnetic excitation. Here the subscript m stands for monochromator, s for sample, and a for analyzer.

Method of measurements

Prior to any elastic and inelastic scattering measurements of the sample, three crucial steps must be done first. Those steps will determine the accuracy and success or failure of the following experiments. The first step is an instrument alignment to achieve the maximum intensity of neutron beam coming to the sample. The second step is a calibration of neutron wavelength to precisely determine the wave vector of the incoming neutron and to set the zero position of the take-off angle of the sample goniometer $2\theta_s$. The third step is a calibration of the energy of the scattered neutrons to determine the right elastic position of the instrument.

The instrument was aligned by optimizing the position of monochromator crystal take-off angle $2\theta_m$, scattering angle θ_m, translational position x_m and y_m, and tilting position Rx_m and Ry_m. The wavelength of the monochromatic neutron was calibrated using a standard sample of silicon powder. The energy of the scattered neutron was calibrated using a sample with a large incoherent scattering cross section, *i.e.*, a vanadium rod with a diameter of 5 mm and a 50 mm height. From the scattered energy calibration, the optimal position of scattering angle and take off angle of the crystal analyzer θ_a and $2\theta_a$, that determine the right elastic position of the instrument were consecutively obtained. Standard techniques of inelastic scattering measurements, *i.e.*, constant momentum transfer **Q** with fixed incoming neutron energy E_i = 30.59 meV and constant transfer energy E with either fixed incoming neutron energy E_i = 30.59 meV or fixed final neutron energy E_f = 14.7 meV, were applied. For thermal neutrons at energies around 14.7 and 30.59 meV, PG filtering works very effectively to suppress $\lambda/2$ and $\lambda/3$ harmonics and pass almost all λ. The measurements were performed to spot spikes of longitudinal magnon in [00ζ], [ζζ0], and [ζζζ] directions.

RESULTS AND DISCUSSION

Figures 1 and 2 represent examples of the results of constant-energy scans in [110] direction with fixed incoming neutron energy of a magnon around (110) Brillouin zone center. The energy transfers are 2.5 and 5 meV, respectively. In Figure 1, two spin waves at symmetrical points about the zone center with very high intensities were observed. The two peaks were observed in both focusing and defocusing sides of the reciprocal space.

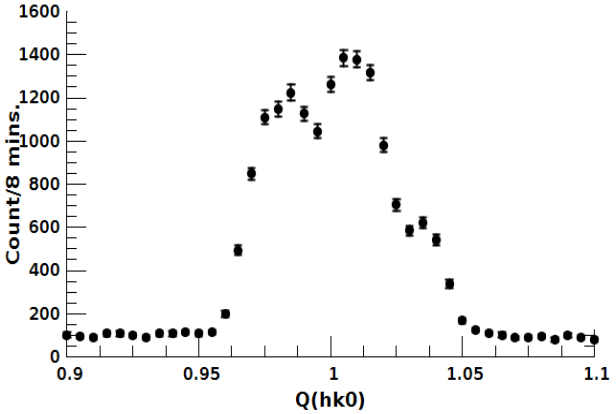

Fig. 1. Result of constant-energy transfer $\hbar\omega$ = 2.5 meV scan with fixed incoming neutron energy = 30.59 meV around (110) Brillouin zone center at room temperature, without PG filter.

For energy transfer of 5 meV, two spin waves at symmetrical positions about the zone center, *i.e.*, Q(0.965, 0.965, 0) and Q(1.03, 1.03, 0) with much lower intensities compared to $\hbar\omega$ = 2.5 meV are observed. In addition, two more peaks are also observed. The author is still not sure about whether these two additional very broad and low-intensity peaks are merely counting from background, phonon, or signals coming from spurions. Further studies need to be performed.

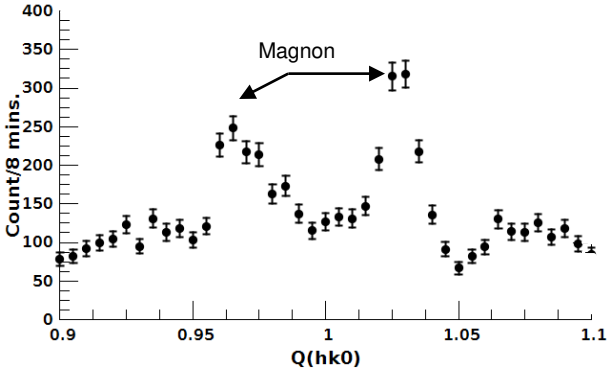

Fig. 2. Result of constant-energy transfer $\hbar\omega$ = 5meV scan with fixed incoming neutron energy = 30.59 meV around (110) Brillouin zone center at room temperature, without PG filter.

An example of constant-energy scan result with fixed neutron E_i for a magnon around (002)

Brillouin zone center is shown in Fig. 3. The energy transfer is 12 meV. Since the magnon was scanned along the longitudinal direction measured from the reciprocal lattice center, both kinds of excitations, *i.e*. longitudinal acoustic LA phonon and magnon, can be simultaneously observed. Two phonons at symmetrical positions of Q(0, 0, 1.85) and Q(0, 0, 2.15) and two magnon at Q(0, 0, 1.95) and Q(0, 0, 2.07) appeared with different heights and widths as the effect of focusing and defocusing due to the shape of resolution function of instrument configuration. For W configuration as SN1 has, the focusing region will be found if the measurement is performed in the direction to the right of the relevant Brillouin zone center.

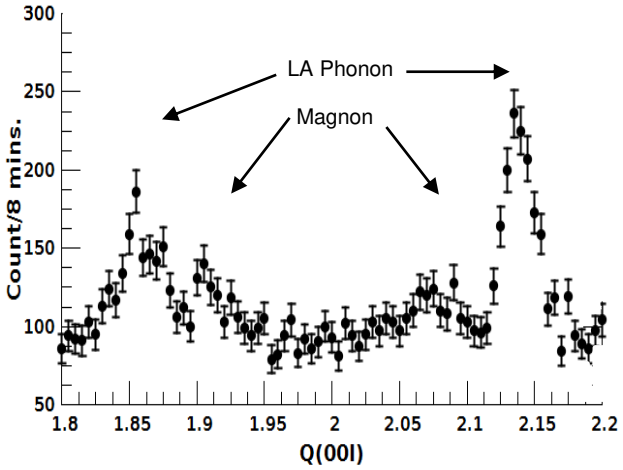

Fig. 3. Result of constant-energy transfer $\hbar\omega$ = 12 meV scan with fixed incoming neutron energy = 30.59 meV around (002) Brillouin zone center at room temperature, without PG filter.

The result of a constant-energy scan with fixed final neutron energy of a longitudinal magnon around (002) Brillouin zone center is shown in Fig. 4. As for measurement with fixed incoming neutron energy scanning, both kinds of excitations, *i.e*., longitudinal acoustic phonon and magnon, were observed. Peaks in Fig. 4 have lower and broader profiles compared to the ones resulting from the measurement with fixed incoming neutron energy as shown in Fig. 3. This is because for present experiment configuration, the method of fixed final neutron energy scan measured excitations at the positions out of the optimal range of scattering angle for PG(002) monochromator crystal of SN1.

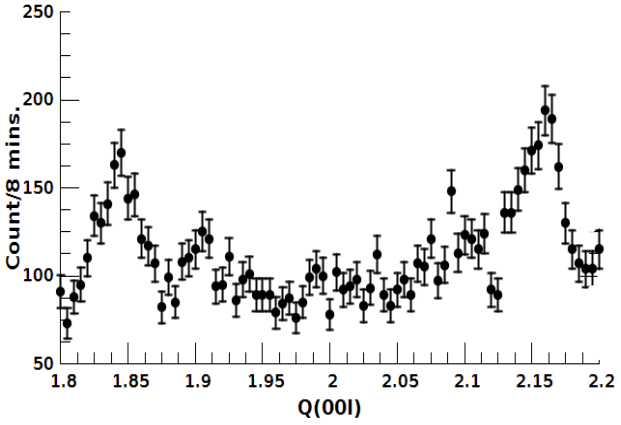

Fig. 4. Result of constant-energy transfer $\hbar\omega$ = 12 meV scan with fixed final neutron energy = 14.7 meV around (002) Brillouin zone center at room temperature, without PG filter.

Figure 5 also shows results of measurement with constant-energy scan with fixed final neutron energy of a longitudinal magnon around (002) Brillouin zone center. The difference between the data presented in Fig. 5 with the one shown in Fig. 4 is that the data in Fig. 5 were obtained in which a PG filter was placed between sample and analyzer. With a PG filter set, the intensities of both kinds of excitations are lower compared with the configuration without PG filter (Fig. 4). The author suspects that this is due to the non-optimal set up of the filter and loss of neutron due to absorption by the filter.

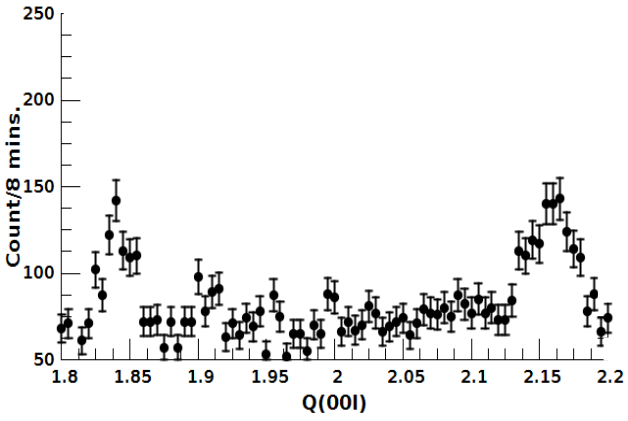

Fig. 5. Result of constant-energy transfer $\hbar\omega$ = 12 meV scan with fixed final neutron energy = 14.7 meV around (002) Brillouin zone center at room temperature, with PG filter after the sample.

Figure 6 shows the result of a constant-energy scan with fixed incoming neutron energy taken from [14]. For both excitations of phonon and magnon the intensity and the resolution of the peaks are respectively much higher and sharper compared with results of present work. At least there are three

reasons regarding this differences in the quality of the data. *i.e*., the flux of the incoming neutron beam of the reference is dozens or even hundreds time more powerful, dimension of the sample is four times larger, and the signal to noise ratio in the reference is very much lower compared with that in the SN1.

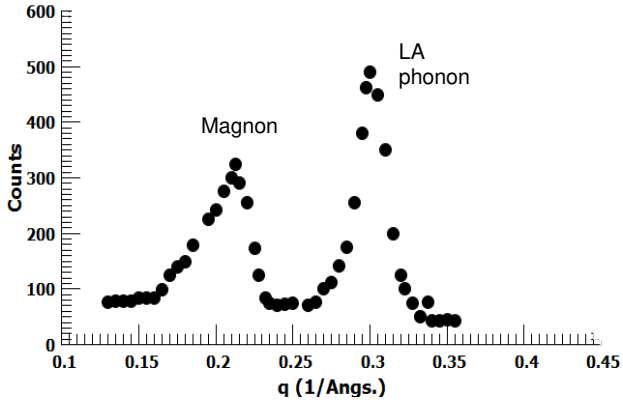

Fig. 6. Result of constant-energy transfer $\hbar\omega$ = 12 meV scan of spin waves (M-magnon) and longitudinal acoustic (LA) phonons at 295 K with fixed incoming energy = 30 meV [14].

In Fig. 7 the results of a constant-**Q** scan with fixed incoming neutron energy of a longitudinal magnon around (110) Brillouin zone center is shown. For very low energy excitation and small wave vector **q**, the intensity of excitations is very strong since the intensity is proportional to 1/q. From Fig. 7, at this particular value of Q the energy of the magnon is about 1.2 meV and for the phonon it is about 2 meV. At these energies, the line of linear acoustic longitudinal phonon is still above the position of magnon dispersion line (see Fig. 10); it explains that for the same Q, the position of LA phonon peak is on the right side (higher energy) of the magnon peak (lower energy).

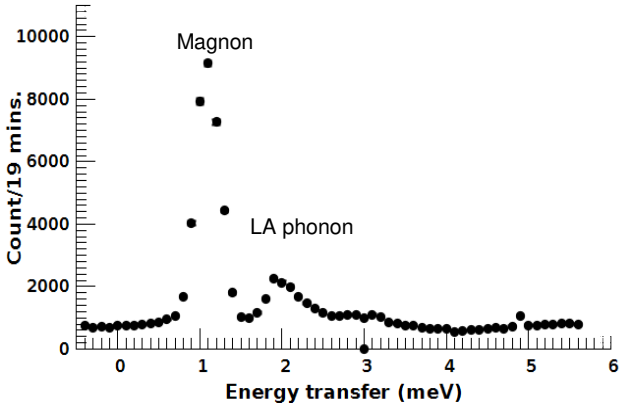

Fig. 7. Result of constant-momentum transfer **Q** scans in [ζζ0] direction at fixed Q(1.035, 1.035, 0) and fixed incoming neutron energy around (1,1,0) Brillouin zone center, without PG filter.

Another example of the results of a constant-**Q** scan with fixed incoming neutron energy of a magnon in [ζζ0] direction is shown in Fig. 8. The measurements were also performed near to (110) Brillouin zone center. The solid dots represent the data taken from experiments and the solid line represents their Gaussian fit. The spin wave energy is about 23 meV. The counting time was 10 minutes for each point. The long counting time increases the background significantly. Nevertheless, it can be seen from the figure that the magnon is still well resolved.

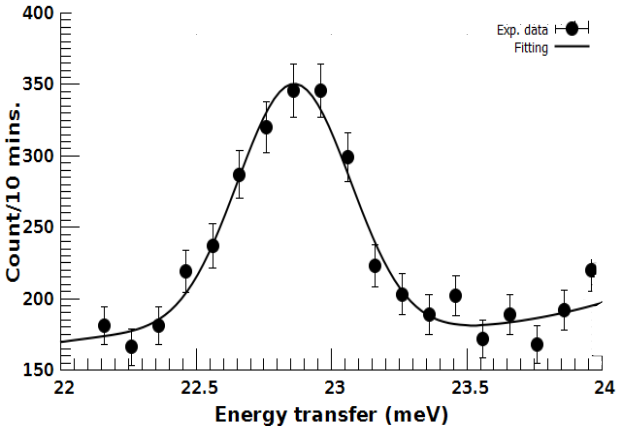

Fig. 8. Result of constant-momentum transfer **Q** scans in [ζζ0] direction at fixed Q (1.09, 1.09, 0) and fixed incoming neutron energy in around (110) Brilouin zone center. The spin wave energy is about 23 meV.

The data of spin wave from present measurements is plotted in a curve of dispersion relation and is shown in Fig. 9. Due to the limitation of instrument configuration of present experiments, the range of spin wave energy that could be measured is only $0 < E < 30$ meV. From the figure, it can be seen that the model of magnetic interaction in Fe (solid triangle) matches the data from measurements (solid circle) relatively well. The model used to fit the data in Fig. 8 is represented by the following equations:

$$\hbar\omega = C + Dq^2\left(1-\beta q^2\right) \qquad D = 2JSa^2 \tag{1}$$

Where,

$$C = 0.15meV, D = 281\pm 10meV \qquad \beta = 1.0Angs.^2 \tag{2}$$

In equation (1), $\hbar\omega$ is energy, C is a constant, D and β are dispersion parameters, q is wave vector, J is the exchange interaction, S is spin magnetic, and a is the lattice constant of *bcc* Fe. All parameters are taken from [14].

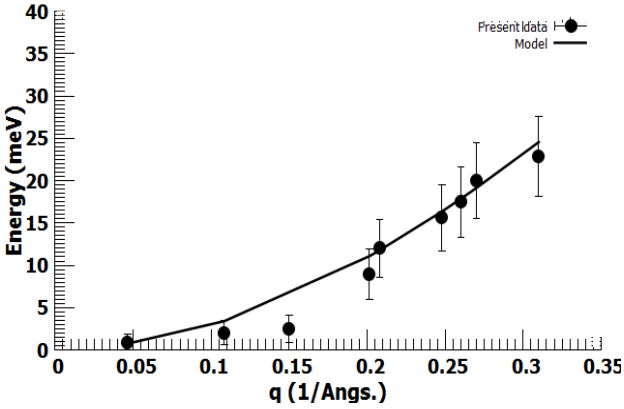

Fig. 9. Spin wave dispersion relation of Fe at room temperature. Comparison between experiments of SN1 (solid circle) and model (solid line).

For comparison, the dispersion relation measured by other investigator [14] is shown in Fig. 10. The dashed line is the same model used to fit the SN1 data (eqs. (1) and (2)). By inspecting the two dispersion curves, it can be concluded that the data resulted from SN1 is in a relatively good agreement with the data taken by Shirane *et al*. [14].

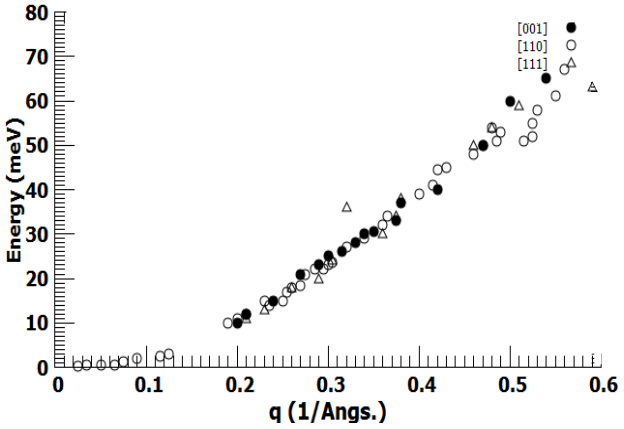

Fig. 10. Spin wave dispersion relation of Fe at 295 K measured in three primary directions [14].

As with the results of magnon measurements, the data of longitudinal acoustic phonon of present works are also in good agreement with the values of the reference [15].

OUTLOOK

There are at least three observations that could be made from the results of the present work. First, currently SN1 is operated with flat single crystals for both monochromator and analyzer. A combination of a very small effective beam size and flat crystals produces a very low intensity that makes real experiments with real samples difficult to perform. Second, the present results show that the background counting is still quite high, giving a very low signal-to-noise ratio. Therefore, it will be difficult for the signals of weak excitations to be identified. Third, all measurements were done at room temperature, whereas interesting phenomena usually appear at extreme conditions such as at very low temperatures.

To gain a higher intensity, focusing systems for monochromator and analyzer are being developed. From focusing monochromator, we expect to increase the intensity by three times, while from focusing analyzer the expectation is about five times. Therefore, a total of fifteen-fold improvement in the intensity of neutron beam will be achieved compared to what is attainable by the present configuration. Increasing the intensity will reduce experimental times significantly and permit investigations of samples with smaller volumes. In addition to present shielding, new shielding systems are being installed around the areas that are suspected as the sources of background. The new shielding is expected to suppress the count coming from unwanted thermal neutron. We are planning to insert sapphire filters before the monochromator to also reduce background levels caused by epithermal and fast neutrons. The background resulting from the present configuration is about 7 counts/minute. With the new shielding we expect to decrease it to 2 or 3 counts/minute. With such a low background, we expect to attain much better signal-to-noise ratios and be able to clearly identify even very weak excitations. Starting this year, the instrument is gradually being equipped with sample environmental control, *i.e*., cryostat, to make SN1 ready for temperature-dependent measurements to investigate interesting and important phenomena that only occur at very low temperatures. We also plan to develop an adjustable external magnetic field device around the sample table for the investigation of magnetic-field-dependent phenomena. At the same time, we have also to think about the resolution width ($\Delta\mathbf{Q}$, ΔE) of the data of our instrument.

CONCLUSION

After more than 20 years since its installation, BATAN's neutron Triple Axis Spectrometer has successfully measured the first magnetic excitation in a single crystal of magnetic material. However, present results have not yet shown good quality of data for standard inelastic scattering measurement. Nevertheless, by simultaneously increasing the intensity, decreasing the background, equipping the

instrument with proper environmental control, and trading the intensity against resolution in the most practical way, SN1 will become BATAN's TAS with a quality that meets standard scientific needs.

ACKNOWLEDGMENT

This work is supported financially by BATAN Research Project (DIPA) 2015. The author would like thank his colleagues Edy Santoso, Rifai M., Bharoto, Sairun, A. Rachmadani, M. Saparudin, Junaedi, Irfan H., and Indarto P. U. for their valuable contributions during the SN1 revitalization process. Special appreciation is addressed to Rifai M. for his helps during sample prealignment. This works is also fully supported by the Head of the Departement of Neutron Beam Technology and the Director of Center for Sciences and Technology of Advanced Materials BATAN. The author also addresses his gratitude to: Prof. Dr. Taku J. Sato of IMRAM, Tohoku University, Japan; Dr. Kirrily Rule of ANSTO, Australia; Dr. Astrid Schneidewind, Dr. Petr Cermak, and Dr. Yixi Su of JCNS - FRM II Germany; Prof. Bruce D. Gaulin of the Department of Physics, McMaster University, Canada; Dr. Martin Boehm of ILL, France; and Dr. Uwe Stuhr of PSI, Switzerland, for their very helpful and valuable discussions and suggestions on magnetic inelastic scattering experiments.

REFERENCES

1. G. Shirane, S.M. Shapiro and J.M. Tranquada, Neutron Scattering with Triple-Axis Spectrometer, Cambridge University Press, Cambridge (2002) 55.
2. B.P. Dalla, M. Mourigal, N. Christensen *et al*., Nat. Phys. **11** (2015) 62.
3. M. Mourigal, E. Mechthild, A. Kloepperpieper *et al*., Nat. Phys. 9 num. **7** (2013) 435.
4. C. Rudowicz and M. Lewandowska, J. Alloys Compd. **540** (2012) 279.
5. Shin-ichi Shamoto, Solid State Commun. **152**, (2012) 653.
6. I. Mirebeau and S. Petit, J. Magn. Magn. Mater. **350** (2014) 209.
7. D. Colognesi, L. Ulivi, M. Zoppi *et al.*, J. Alloys Compd. **538** (2012) 91.
8. S.K. Callear, A.J. Ramirez-Cuesta, W.I.F. David *et al*., Chem. Phys. **427** (2013) 9.
9. K. Sumida, C.M. Brown, Z.R. Herm *et al.*, Chem. Commun. **47** (2011) 1157.
10. K. Kamazawa, M. Aoki, Noritake *et al.*, Adv. Energy Mater. **3** (2013) 39.
11. J.A. Schneeloch, Z. Xu, J. Wen *et al*., Phys. Rev. B **91** (2015) 064301.
12. J.D. Nickels, H. O'Neill, L. Hong *et al*., Biophys. J. **103** (2012) 1566.
13. J.D. Nickels, S. Perticaroli, H. O'Neill *et al*., Biophys. J. **105** (2013) 2182.
14. G. Shirane, V.J. Minkiewicz and R. Nathans, J. Appl. Phys. **39** (1968) 383.
15. B.N. Brockhouse, H.E. Abou-Helal and E.D. Hallman, Solid. State Commun. **5** (1967) 211.